Short communication

Optimization of Ni^{2+}/Ni^{3+} ratio in layered $Li(Ni,Mn,Co)O_2$ cathodes for better electrochemistry

N.V. Kosova [a,*], E.T. Devyatkina [a], V.V. Kaichev [b]

[a] *Institute of Solid State Chemistry and Mechanochemistry SB RAS, ul. Kutateladze 18, 630128 Novosibirsk, Russia*
[b] *Boreskov Institute of Catalysis SB RAS, pr. Acad. Lavrent'eva 5, 630090 Novosibirsk, Russia*

Abstract

A study of the $LiNi_{1-x-y}Co_xMn_yO_2$ ($x = y = 0.1$; 0.2; 0.33) cathode materials prepared from mixed hydroxides and LiOH using the method of mechanical activation has been performed. All as prepared materials were indexed in the R-$3m$ space group. The cell volume and the degree of structural disordering decrease with reducing of Ni content. According to XPS study, the main electronic state of d-ions in the surface layer of particles corresponds to Ni^{2+}, Co^{3+} and Mn^{4+}. However, the $Ni2p_{3/2}$ and $Co2p_{3/2}$ binding energy increases versus Ni content, indicating the increased Me—O bond covalency. The highest specific discharge capacity was observed for $LiNi_{0.6}Co_{0.2}Mn_{0.2}O_2$—170 mAh g^{-1}. The position of redox peaks on the differential capacity curves depends on the composition of the sample: it shifts towards lower voltage with increased Ni content.
© 2007 Elsevier B.V. All rights reserved.

Keywords: Lithium-ion batteries; Layered Ni-based cathodes; Mechanical activation; Ni^{2+}/Ni^{3+} ratio; XPS study; Electrochemical study

1. Introduction

Researchers worldwide are searching for high-capacity, safe, and inexpensive replacement for $LiCoO_2$. Layered $LiNi_{1-x-y}Co_xMn_yO_2$ cathodes are more attractive from the point of view of higher capacity, reduced capacity fades and high-rate performance [1–11]. Some researchers study Ni-rich compositions considering them as $LiNiO_2$ substituted solid solutions ([Ni] ≫ [Mn], [Co]). The others investigate solid solutions in the $xLiNi_{1/2}Mn_{1/2}O_2$–$yLiCoO_2$ system with [Ni] = [Mn]. Another group of solid solutions in the $xLiNi_{1/2}Mn_{1/2}O_2$–$yLiCoO_2$–zLi_2MnO_3 system with [Ni] < [Mn] represents Mn-excess cathodes. In the $xLiNi_{1/2}Mn_{1/2}O_2$–$yLiCoO_2$ solid solutions, Ni ions are preferably in 2+ oxidation state, while in the $LiNiO_2$ substituted solutions, they should be both in 2+ and 3+ state (Table 1). It is widely accepted that redox reaction takes place between Ni^{2+} and Ni^{4+}. However, large amount of Ni^{2+} ions with big ionic radius can lead to their partial transfer to Li sites (cationic mixing) worsening electrochemical properties. Optimized Ni^{2+}/Ni^{3+} ratio is necessary for better electrochemistry of $LiNi_{1-x-y}Co_xMn_yO_2$ cathodes.

To improve cyclability and to increase rate capability of cathode materials, smaller particles are needed since they are more flexible for lithium insertion–extraction than larger particles. Furthermore, during cycling, the changes in the lattice parameters do not affect the cyclability of smaller particles to the degree that larger particles are affected. Mechanical activation is a promising route to prepare high-dispersed cathode materials.

In the present study, the properties of Ni-based solid solutions $LiNi_{1-x-y}Co_xMn_yO_2$ ($0.1 \le x, y \le 1/3$) with different Ni^{2+}/Ni^{3+} ratio synthesized using mixed hydroxides and mechanical activation (MA) method were studied.

2. Experimental

Mixed Ni–Co–Mn hydroxides with correspondent composition and LiOH were used as reagents. Preliminary MA was performed in high-energetic planetary mill AGO-2 for 1–10 min. The reactions of hydroxides under MA are called '*soft mechanochemical synthesis*' [12]. As prepared precursors were shortly heat treated at 800–900 °C in air. Crystal and local structure of the materials was studied by X-ray powder diffraction (DRON-3M diffractometer, Cu Kα radiation) and IR spectroscopy (Bruker FTIR spectrometer, pellets with CsI, 200–4000 cm^{-1}). Electronic state of ions was investigated using XPS spectroscopy (VG ESCALAB HP spectrometer,

* Corresponding author. Tel.: +7 383 3363843; fax: +7 383 3322847.
E-mail address: kosova@solid.nsc.ru (N.V. Kosova).

Table 1
Theoretical capacity for some $LiNi_{1-x-y}Co_xMn_yO_2$ cathodes

Composition	[Ni^{2+}] per formula	[Ni^{3+}] per formula	Number of electrons to be donated	$Q_{theor.}$[a] (mAh g^{-1})	Refs.
$LiNi_{1/3}Co_{1/3}Mn_{1/3}O_2$	0.33	–	0.66	183	[1]
$LiNi_{0.4}Co_{0.2}Mn_{0.4}O_2$	0.40	–	0.80	223	[6]
$LiNi_{0.425}Co_{0.15}Mn_{0.425}O_2$	0.425	–	0.85	237	[7]
$LiNi_{0.5}Co_{0.25}Mn_{0.25}O_2$	0.25	0.25	0.75	208	[8]
$LiNi_{0.6}Co_{0.2}Mn_{0.2}O_2$	0.20	0.4	0.80	221	[9]
$LiNi_{0.7}Co_{0.2}Mn_{0.1}O_2$	0.10	0.6	0.80	220	[10]
$LiNi_{0.8}Co_{0.1}Mn_{0.1}O_2$	0.20	0.7	0.90	248	[11]

[a] Assuming that only Ni ions are oxidized.

Al $K\alpha$ radiation, $h\nu = 1486.6$ eV). Electrochemical tests were performed in laboratory cells with the $LiPF_6 + EC + DMC$ electrolyte and Li anode in the 2.5–4.3 V range at current density of 0.155 mA cm^{-2} and $T = 20\,^{\circ}$C. Cathodes were prepared by mixing active material with 15% Super P (TIMCAL Ltd.).

3. Results and discussion

Activated mixtures were air-light powders and were easily extracted form the jars. Fig. 1 shows X-ray patterns of the mixed $Ni_{1/3}Co_{1/3}Mn_{1/3}(OH)_2$ hydroxide (S.g. P-$3m1$) and the products of its interaction with LiOH under MA and subsequent heat treatment at 400 and 850 $^{\circ}$C. One can see that low crystallized product with layered structure is already formed at 400 $^{\circ}$C. Under higher temperature, the completion of the structure formation and the product crystallization occur.

According to X-ray analysis, as prepared products were phase-pure solid solutions with layered structure, S.g. R-$3m$. Cell parameters a and c as well as cell volume are shown in Table 2.
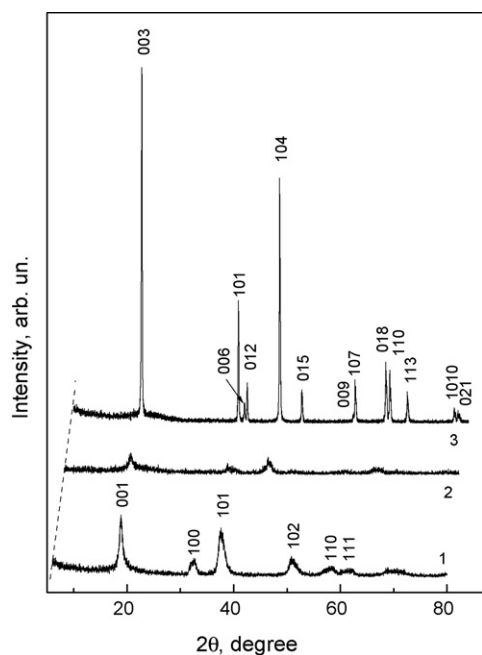
They are increased at higher temperatures evidencing possible reduction of Ni and Mn ions. $LiNi_{1/3}Co_{1/3}Mn_{1/3}O_2$ shows the lowest cell volume. The c/a and I_{003}/I_{104} ratio indicates that the degree of cation mixing increases versus Ni content and the heating temperature. The latter is induced by partial migration of Ni^{2+} ions in Li sites.

IR spectra confirm the layered structure of all as prepared samples (Fig. 2). The intensity of LiO_6 and MO_6 bands increases with decreased Ni content. The shift to higher frequency range is also observed, probably to decrease of Me–O covalency [13]. In the spectra of Ni-rich samples, the vibration bands of CO_3^{2-} groups are present.

The results of XPS study are shown in Fig. 3 and Table 3. The Ni2p spectra of as prepared samples are characterized by two main lines Ni2p$_{3/2}$ and Ni2p$_{1/2}$ and two intensive shake-up satellites S_1 and S_2 characteristic of Ni^{2+} ions [14–16]. However, a noticeable shift of maximum of the Ni2p$_{3/2}$ line to higher binding energy was observed with increasing Ni content. The close value of binding energy was detected for $LiNiO_2$ and attributed to Ni^{3+} ions based on the simple ionic model [17].

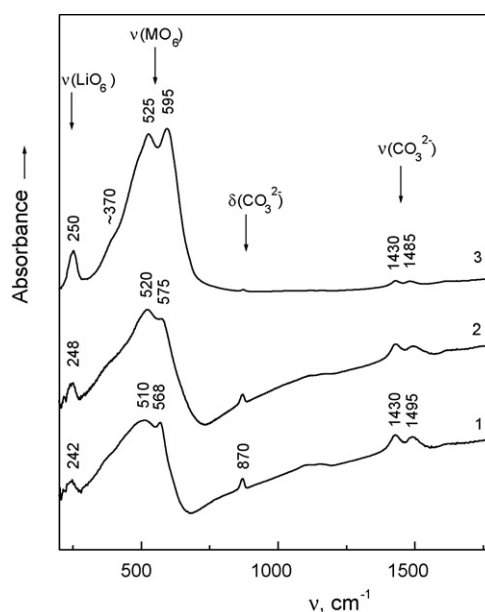Fig. 1. X-ray diffraction patterns of $Ni_{1/3}Co_{1/3}Mn_{1/3}(OH)_2$ (1), the products of its interaction with LiOH under MA and heat treatment at 400 $^{\circ}$C (2) and 850 $^{\circ}$C (3).

Fig. 2. IR spectra of $LiNi_{0.8}Co_{0.1}Mn_{0.1}O_2$ (1), $LiNi_{0.6}Co_{0.2}Mn_{0.2}O_2$ (2) and $LiNi_{1/3}Co_{1/3}Mn_{1/3}O_2$ (3) prepared at 850 $^{\circ}$C.

Table 2
Cell parameters of as prepared $LiNi_{1-x-y}Co_xMn_yO_2$

Composition	T (°C)	Cell parameters		c/a	V (Å^3)	I_{003}/I_{104}
		$a \pm 0.0005$ (Å)	$c \pm 0.003$ (Å)			
$LiNi_{0.8}Co_{0.1}Mn_{0.1}O_2$	800	2.8822	14.226	4.936	102.34	1.13
	850	2.8841	14.234	4.936	102.53	1.02
	900	2.8896	14.249	4.931	103.03	0.75
$LiNi_{0.6}Co_{0.2}Mn_{0.2}O_2$	800	2.8673	14.213	4.957	101.19	1.45
	850	2.8685	14.218	4.957	101.32	1.47
	900	2.8721	14.228	4.954	101.64	1.18
$LiNi_{1/3}Co_{1/3}Mn_{1/3}O_2$	800	2.8596	14.221	4.973	100.71	1.42
	850	2.8585	14.222	4.975	100.64	1.43
	900	2.8603	14.228	4.974	100.81	1.38
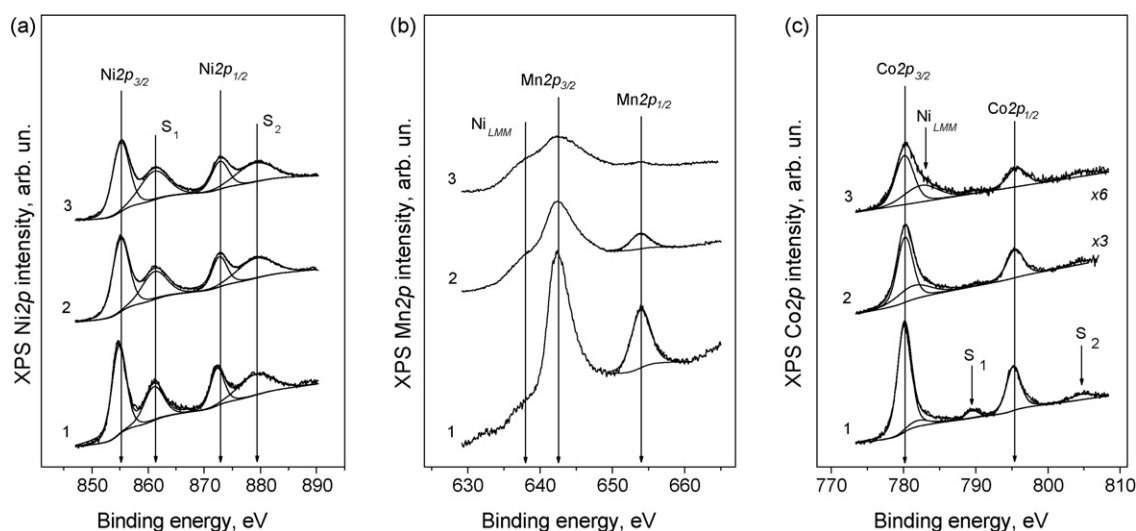
Fig. 3. Ni2p (a), Mn2p (b) and Co2p (c) XPS spectra of $LiNi_{1/3}Co_{1/3}Mn_{1/3}O_2$ (1), $LiNi_{0.6}Co_{0.2}Mn_{0.2}O_2$ (2) and $LiNi_{0.8}Co_{0.1}Mn_{0.1}O_2$ (3). All spectra are normalized on intensity of correspondent Ni2p spectrum. The binding energies were calibrated against the C1s line of hydrocarbon admixtures (284.8 eV).

The analysis of the Mn2p spectra is hampered by its overlapping with the $NiL_3M_{23}M_{45}$ Auger spectrum and by low concentration of surface Mn. However, comparing the observed binding energies with those for different Mn oxides [6,18,19], one can conclude that Mn in $LiNi_{1-x-y}Co_xMn_yO_2$ is preferably in 4+ state.

In the Co2p spectra, two sharp peaks Co2p$_{3/2}$ and Co2p$_{1/2}$ at 780.1 and 795.1 eV and two low-intensive shake-up satellites at 789.5 and 804.6 eV are observed. Such a spectrum is a characteristic of LiCoO$_2$ [14,20]. As in the case of Ni2p$_{3/2}$ spectra, an increase of Ni content leads to a slight shift of Co2p$_{3/2}$ to higher binding energy. The corresponding effect of Co and Mn content on the Ni2p$_{3/2}$ binding energy was also observed by other authors [8,21]. One of the possible explanations is the changing of the Me–O bond covalency that is confirmed by IRS data (Fig. 2). According to EXAFS [22], the increased Mn content in $LiNi_{0.75-y}Co_{0.25}Mn_yO_2$ does not noticeably change the M–O and M–M (M = Co, Mn) bonds as well as the Co and Mn charge state, but the Ni–O bond length increases.

Estimation of Me ion content on the surface of the particles indicates the process of Ni ion segregation (Table 3). On contrary, the surface is poor with Mn ions. Actually, the chemical

Table 3
Binding energy (eV) and relative atomic concentration in as prepared $LiNi_{1-x-y}Co_xMn_yO_2$

	$LiNi_{0.33}Co_{0.33}Mn_{0.33}O_2$	$LiNi_{0.6}Co_{0.2}Mn_{0.2}O_2$	$LiNi_{0.8}Co_{0.1}Mn_{0.1}O_2$
Ni2p$_{3/2}$	854.6	855.1	855.2
Co2p$_{3/2}$	780.1	780.2	780.4
Mn2p$_{1/2}$	642.4	642.5	–
[Co]/[Ni]	0.70	0.21	0.10
[Mn]/[Ni]	0.95	0.17	0.02
[O]/[Ni + Co + Mn]	4.0	5.7	8.6
[CO$_3$]/[Ni + Co + Mn]	0.15	0.85	2.4

content of the surface and of the bulk is markedly different. The same effect was observed for the $LiNi_{1-x}Mn_xO_2$ solid solutions [13].

According to C1s and O1s spectra (not shown here), with increasing Ni content, the amount of carbonate surface groups also increases, which is correlated with IRS data. Indeed, the features at 284.8 and 289.5 eV are detected in the C1s spectra. The first, more intensive, corresponds to carbon in hydrocarbon impurities, while the second one—to carbon in carbonate groups. However, taking into account surface carbonate formation, relative atomic concentration of O/d-metal exceeds stoichiometric values (see Table 3). One can suppose that a part of surface O is present in the state with lower electronic state, e.g. $O^{-\delta}$ characterized by higher value of binding energy. In the O1s spectra, two features at 529.3 and 531.4 eV are really observed. The first one can be assigned to lattice oxygen and the second—to oxygen in carbonate group and $O^{-\delta}$.

Thus, electronic state of Ni and O ions noticeably changes versus Ni content in $LiNi_{1-x-y}Co_xMn_yO_2$ due to increase of Ni–O covalency.

It is worth noticing, that we did not observe the lines correspondent to Fe in spite the samples were prepared by MA with stainless jars and balls. This confirms that MA in the mixtures of hydroxides is indeed realized under mild conditions excluding contamination [12].

Charge–discharge curves (Fig. 4) show low polarization and low ohmic resistance—characteristic of high-dispersed materials. The specific discharge capacity versus cycle number for materials with different composition is represented in Fig. 5. The highest capacity ($170\,mAh\,g^{-1}$) was observed for the $LiNi_{0.6}Co_{0.2}Mn_{0.2}O_2$ sample. The capacity of $LiNi_{0.8}Co_{0.1}Mn_{0.1}O_2$ was significantly lower than the theoretical one, most probably, due to cation mixing (see X-ray data) and surface admixtures (see XPS data).

Fig. 6 shows the differential capacity curves. Only one oxidation and one reduction peaks are observed, contrary to $LiNiO_2$. However, for $LiNi_{0.8}Co_{0.1}Mn_{0.1}O_2$, low-intensive non-reversible oxidation peak at 4.08 V appears at the first cycle. The minimum difference between oxidation and reduction peaks was observed for $LiNi_{0.6}Co_{0.2}Mn_{0.2}O_2$ with theoretical ratio $Ni^{2+}/Ni^{3+} = 1/2$. The average discharge potential depends on the sample composition and comprises 3.75, 3.71

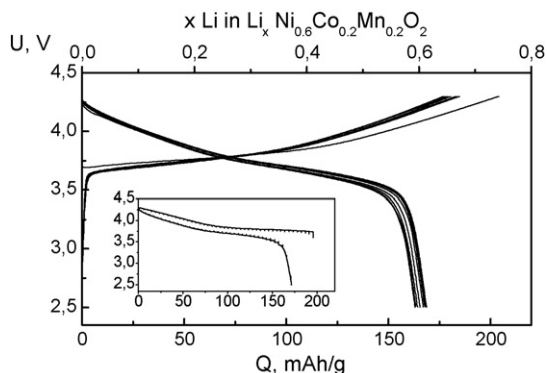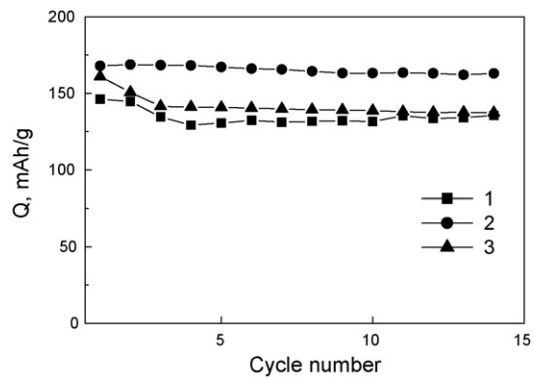Fig. 4. Charge–discharge curves of $LiNi_{0.6}Co_{0.2}Mn_{0.2}O_2$. ITT curve is shown in the insert.

Fig. 5. Discharge capacity vs. cycle number: $LiNi_{0.8}Co_{0.1}Mn_{0.1}O_2$ (1), $LiNi_{0.6}Co_{0.2}Mn_{0.2}O_2$ (2) and $LiNi_{1/3}Co_{1/3}Mn_{1/3}O_2$ (3) ($T = 850\,^\circ C$).
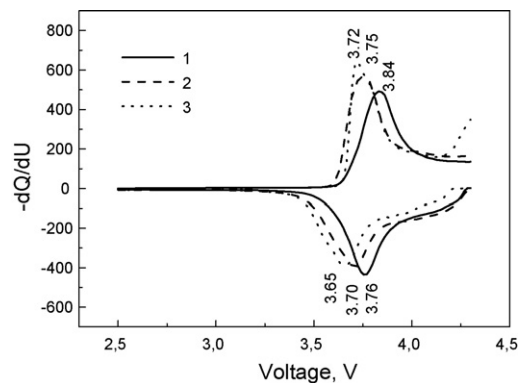
Fig. 6. Differential capacity curves for $LiNi_{1/3}Co_{1/3}Mn_{1/3}O_2$ (1), $LiNi_{0.6}Co_{0.2}Mn_{0.2}O_2$ (2) and $LiNi_{0.8}Co_{0.1}Mn_{0.1}O_2$ (3) ($T = 850\,^\circ C$).

and 3.62 V for $LiNi_{1/3}Co_{1/3}Mn_{1/3}O_2$, $LiNi_{0.6}Co_{0.2}Mn_{0.2}O_2$ and $LiNi_{0.8}Co_{0.1}Mn_{0.1}O_2$, respectively. Thus, charge–discharge capacity depends on the Ni^{2+}/Ni^{3+} ratio in cathode material and on the Me–O bond covalency.

4. Conclusions

It has been shown that the method of mechanical activation can be successfully used to prepare $LiNi_{1-x-y}Co_xMn_yO_2$ cathode materials starting from mixed Ni, Co, Mn hydroxides and LiOH. As prepared materials with $x = y = 0.1$; 0.2; 0.33 differ by the degree of structural ordering and electronic state of d-ions: cation mixing and Me–O bond covalency increase versus Ni content. This influences the capability, the value of specific capacity and the position of redox peaks for these cathode materials.

References

[1] N. Yabuuchi, T. Ohzuku, J. Power Sources 119–121 (2003) 171.
[2] Y. Koyama, Y. Makimura, I. Tanaka, H. Adachi, T. Ohzuku, J. Electrochem. Soc. 151 (2004) A1499.

[3] Y. Koyama, N. Yabuuchi, I. Tanaka, H. Adachi, T. Ohzuku, J. Electrochem. Soc. 151 (2004) A1545.

[4] N. Yabuuchi, Y. Koyama, N. Nakayama, T. Ohzuku, J. Electrochem. Soc. 152 (2005) A1434.

[5] J. Jiang, K.W. Eberman, L.J. Krause, J.R. Dahn, J. Electrochem. Soc. 152 (2005) A1879.

[6] J.K. Ngala, N.A. Chernova, M. Ma, M. Mamak, P.Y. Zavalij, M.S. Whittingham, J. Mater. Chem. 14 (2004) 214.

[7] N. Tran, L. Croguennec, C. Jordy, Ph. Biensan, C. Delmas, Solis State Ionics 176 (2005) 1539.

[8] P.Y. Liao, J.G. Duh, S.R. Sheen, J. Electrochem. Soc. 152 (2005) A1695.

[9] H. Cao, Y. Zhang, J. Zhang, B. Xia, Solid State Ionics 176 (2005) 1207.

[10] Z. Liu, A. Yu, J.Y. Lee, J. Power Sources 81–82 (1999) 416.

[11] J. Cho, T.-J. Kim, J. Kim, M. Noh, B. Park, J. Electrochem. Soc. 151 (2004) A1899.

[12] E. Avvakumov, M. Senna, N. Kosova, Soft Mechanochemical Synthesis. A Basics for New Chemical Technologies, Kluwer Academic Publishers, Boston, Dordrecht, London, 2001, p. 207.

[13] N. Kosova, E. Devyatkina, V. Kaichev, Lithium Battery Discussion: Electrode Materials, Bordeaux-Arcachon, France, May 2005, p. 50.

[14] N.S. McIntyre, M.G. Cook, Anal. Chem. 47 (1975) 2208.

[15] C.P. Li, A. Proctor, D.M. Hercules, Appl. Spectrosc. 38 (1984) 880.

[16] K.M. Shaju, G.V. Subba Rao, B.V.R. Chowdari, Electrochim. Acta 48 (2003) 1505.

[17] K. Amine, H. Tukamoto, H. Yasuda, Y. Fujita, J. Electrochem. Soc. 143 (1996) 1607.

[18] K.M. Shaju, G.V. Subba Rao, B.V.R. Chowdari, Electrochim. Acta 48 (2003) 145.

[19] M. Oku, K. Hirokawa, S. Ikeda, J. Electron Spectrosc. Relat. Phenom. 7 (1975) 465.

[20] N.V. Kosova, V.V. Kaichev, V.I. Bukhtiyarov, D.G. Kellerman, E.T. Devyatkina, T.V. Larina, J. Power Sources 119–121 (2003) 669.

[21] Y. Sun, C. Ouyang, Z. Wang, X. Huang, L. Chen, J. Electrochem. Soc. 151 (2004) A504.

[22] B.J. Hwang, Y.W. Tsai, C.H. Chen, R. Santhanam, J. Mater. Chem. 13 (2003) 1962.